International Journal on Advanced Science Engineering Information Technology

Vol.6 (2016) No. 6
ISSN: 2088-5334

Analysis of Offset Antennas in Radio Telescopes

Kim Ho Yeap[#], Chorng Yin Yiam[*], Koon Chun Lai[*], Mey Chern Loh[*], Soo King Lim[*], Zairi Ismael Rizman[##]

[#]*Faculty of Engineering and Green Technology, Tunku Abdul Rahman University, Kampar Perak, 31900, Malaysia*
E-mail: yeapkh@utar.edu.my

[*]*Faculty of Engineering and Green Technology, Tunku Abdul Rahman University, Kampar Perak, 31900, Malaysia*
E-mail: yiam919@1utar.my, laikc@utar.my, mcloh87@gmail.com, limsk@utar.edu.my

[##]*Faculty of Electrical Engineering, Universiti Teknologi MARA, Dungun, Terengganu, 23000, Malaysia*
E-mail: zairi576@tganu.uitm.edu.my

***Abstract*— We present an analysis on the performance of two popular dual offset antennas design, i.e. the offset Cassegrain and Gregorian reflector antennas. In our study, we have adopted the design parameters for the Cassegrain configuration used in the Atacama Large Milimeter Array (ALMA) project. Modifications on the original parameters are made so as to meet the design requirement of the offset configurations. To reduce spillover loss, we have adjusted the angle between the axis of the primary reflector and that of the sub-reflector to 0.20^{o}. The results obtained from the physical optics computation show that the amplitude at the main lobe of the Gregorian configuration is approximately 74.02 dB, while that of the Cassegrain configuration is approximately 74 dB. The maximum (relative) side lobe level, SLL_{dB} for the Cassegrain and Gregorian configurations are found as -3.67 dB and -3.69 dB respectively. Although the magnitude of the main lobe for both configurations is comparable, the Gregorian antenna gives relatively lower SLL_{dB}. In other words, the Gregorian configuration performs relatively better than its Cassegrainian counterpart.**

***Keywords*— reflector antennas; Cassegrain offset; Gregorian offset; physical optics; radio telescopes**

I. INTRODUCTION

In ground-based radio astronomy, radio telescopes are built to observe naturally occurring signal emission from cosmic sources, such as stars, galaxies, planet, quasars, etc [1]–[5]. A typical radio telescope consists of a parabolic primary reflector antenna and a hyperboloid or ellipsoid sub-reflector. Incoming signal radiation is collected by both the primary and sub-reflectors and is subsequently focused onto a sensitive receiver located behind or at the bottom of the parabolic reflector. The incoming waves are then converted into electrical signals inside the receiver and processed to display the spectral and spatial information carried by the signal [6]–[8].

The radiation characteristics of a reflector like an antenna efficiency, antenna pattern, polarization discrimination, etc. are highly dependent on the structural configuration of the antenna. Studies have shown that a reflector that uses a parabolic geometry in its design can obtain better radiation characteristics as when compared to those using a corner reflector or a plane reflector [9]. Examples of paraboloid reflector antennas are the front-fed parabolic, Cassegrain, Gregorian, Naysmith, offset Cassegrain and Gregorian as well as the beam waveguide configurations [10]. An offset Cassegrain or Gregorian is a type of asymmetry paraboloid reflector antenna. The configuration of an offset antenna is that the subreflector and feed are placed at one side of the primary reflector. As a result, the focal point of the antenna is also located on the side of the primary reflector. Examples of existing telescopes which employ offset Gregorian optics are the Green Bank Telescope (GBT) [11]–[14], the Arecibo observatory [15], [16] and the Allen Telescope Array (ATA) [17], [18] while the Crawford Hill antenna of the Bell Telephone Laboratories [19], [20] employs the offset Cassegrain configuration. The main advantage of the offset design is that the aperture blockage can be reduced since the feed, subreflector and the support structure are moved away from the path of the incoming signals to the primary reflector. Hence, the loss of the antenna, particularly spillover loss and also cross polarization can be significantly reduced [21]. Fig. 1 (a) and (b) illustrate the optical arrangement of an offset Cassegrain and an offset Gregorian antenna respectively. As compared to the Cassegrain design, it can be seen from Fig. 1 that the position of the subreflector of the offset Gregorian antenna is located somewhat farther from the primary reflector, while the feed is nearer to the subreflector. Because of this reason, the offset Gregorian is relatively larger in size. Since both offset designs have their

own advantages and disadvantages, it will certainly be interesting to find out which design configuration performs better at a particular range of frequency. In this paper, we present an investigation on the radiation characteristics of these two types of offset reflector antennas.

II. Material and Method

In our analysis, we employ the parameters used in [4] for both the offset Gregorian and Cassegrain antennas. To minimize the side lobe levels and cross polarization, we also apply Mizugutchi condition to optimize the design of our offset antennas. The condition to cancel cross polarization in offset designs can be determined by equation [22] as follows

$$M = \frac{|1-e^2|}{(1+e^2)-2e\cos\beta} \tag{1}$$

where M is the magnification ratio, e the eccentricity of the subreflector as depicted in Fig. 1 (a) and (b), β is the angle between the axis of the primary reflector and that of the subreflector. To develop the offset configurations based on the original on-axis designs in [4], β is adjusted to move the positions of the feed and the reflectors.

III. Results and Discussion

To analyze the performance of the offset Cassegrain and Gregorian designs, we have selected signal frequency f at the high edge of ALMA band 1, i.e. 45 GHz. We have also varied β at 0.20°, 0.25°, 0.30° and 0.35°. As shown in Fig. 1 (a) and (b), the smaller the angle of β, the distance of the feed will be shifted closer to the primary reflector. Hence, it is important to ensure that an appropriate value for β is to be chosen. This is to avoid placing the feed underneath the parabolic reflector causing the signal to be partially, if not completely, blocked by the reflector. With careful design, we found that at β = 0.20°, the feed is placed close enough right next to the edge of the parabolic reflector. The parameters for both Cassegrain and Gregorian antennas are tabulated respectively in Table 1 and 2. Fig. 2 to 4 depict the radiation patterns of the offset Cassegrain antenna at ϕ = 0°, 45° and 90° respectively. As can be observed from the figures, the magnitudes of the side lobes for different β values are almost comparable and can hardly be distinguished. On the other hand, the main lobes show a marked difference with β = 0.20° having the highest amplitude. It can also be seen that the amplitude at the main lobe gradually decreases as β increases. Indeed, the results obtained for the case of the Gregorian antenna is in consistency with those found in the Cassegrain antenna. As can be seen in Fig. 5 to 7, although there is no obvious difference among the radiation patterns of the side lobes, the main lobe at the sub-reflector of the Gregorian antenna is at his highest when β = 0.20° and the lowest at β = 0.35°. The results found in both offset configurations are in agreement with each other. As β increases further from 0.20°, the feed will be shifted farther away from the primary reflector. Hence, we attribute the reduction of amplitude at the main lobe, to the increase of spillover effect when the feed is placed farther away from the reflector.

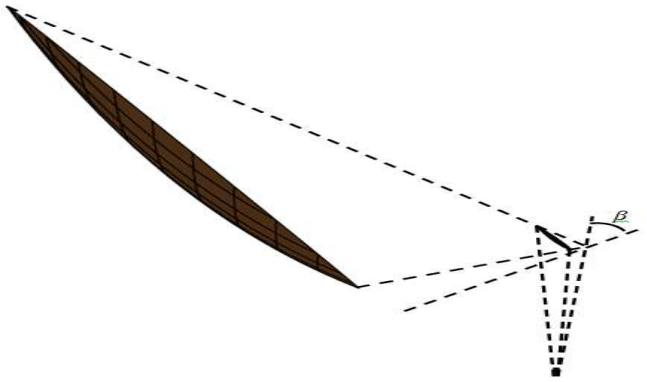

(a)

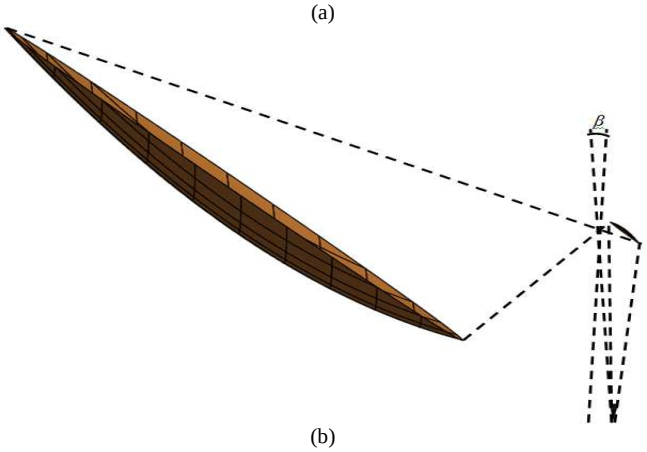

(b)

Fig. 1 The optical arrangement of an (a) offset Cassegrain antenna (b) offset Gregorian antenna

TABLE I
Parameters for The Cassegrain Antenna

Symbol	Description	Data
D	Diameter of primary aperture	12.0 m
f_p	Focal length of primary reflector	4.8 m
d	Diameter of secondary aperture	0.75 m
M	Magnification	20
f/D	Primary focal ratio	0.4
F	Focal length of equivalent paraboloid	96 m
F/D	Secondary focal ratio	8
e	Secondary eccentricity	1.10526
$2c$	Distance between primary and secondary foci	6.177 m
z_f	Back focal distance	1.377 m
β	Angle between main reflector axis and secondary reflector axis	0.20°

TABLE II
Parameters for The Gregorian Antenna

Symbol	Description	Data
D	Diameter of primary aperture	12.0 m
f_p	Focal length of primary reflector	4.8 m
d	Diameter of secondary aperture	0.75 m
M	Magnification	-20
f/D	Primary focal ratio	0.4
F	Focal length of equivalent paraboloid	96 m
F/D	Secondary focal ratio	8
e	Secondary eccentricity	0.90476
$2c$	Distance between primary and secondary foci	6.177 m
z_f	Back focal distance	1.377 m
β	Angle between main reflector axis and secondary reflector axis	0.20°

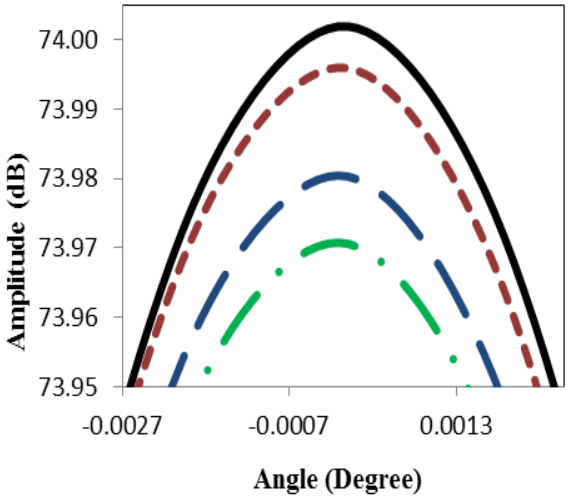

(a)

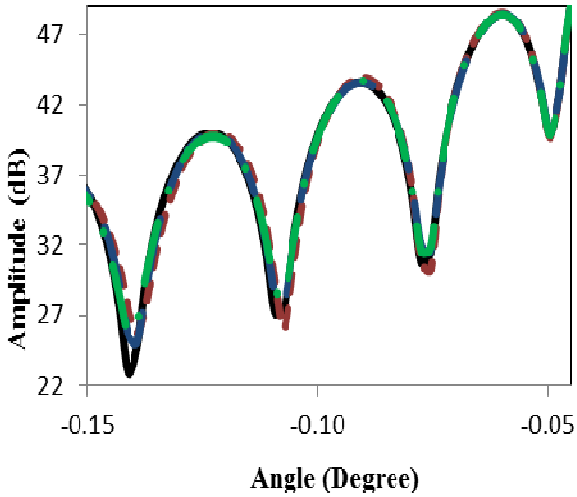

(b)

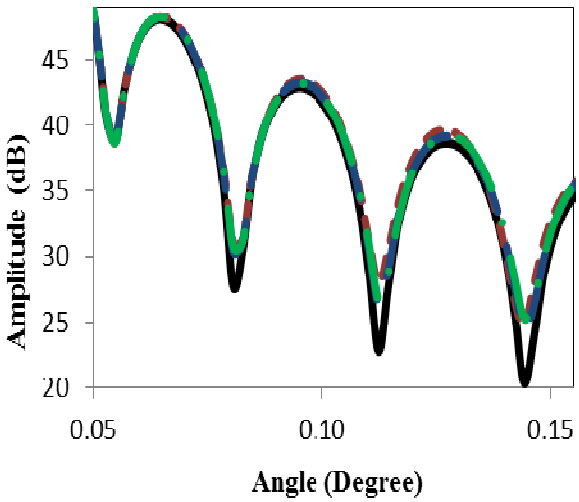

(c)

Fig. 2 The beam patterns of an offset Cassegrain with $\beta = 0.20^{o}$ (solid lines), 0.25^{o} (dotted lines), 0.30^{o} (dashed lines) and 0.35^{o} (dashed-dotted lines) at f = 45 GHz and $\varphi = 0^{o}$. (a) Main lobe (b) side lobes at $\theta = -0.15^{o}$ to -0.045^{o} and (c) side lobes at $\theta = 0.045^{o}$ to 0.15^{o}

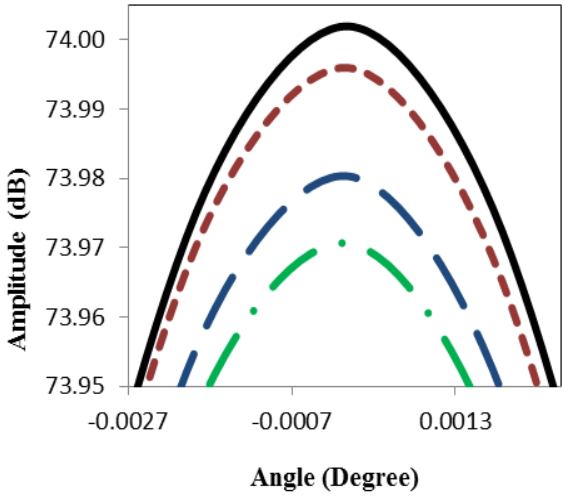

(a)

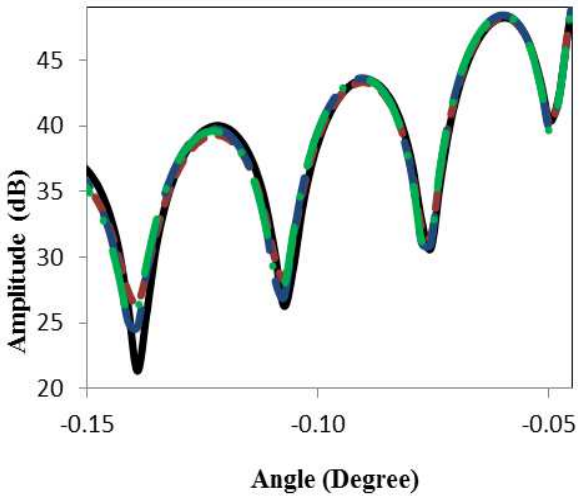

(b)

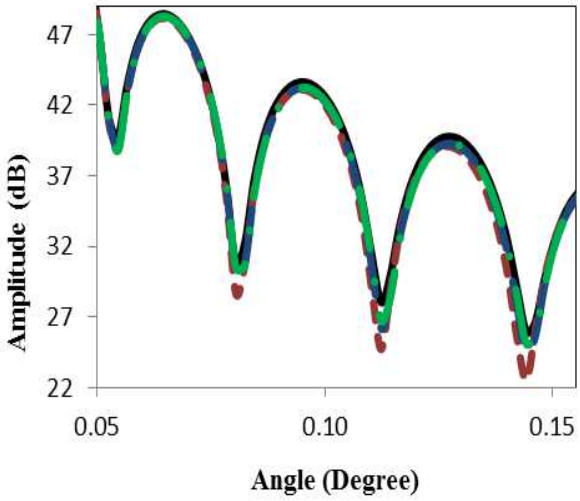

(c)

Fig. 3 The beam patterns of an offset Cassegrain with $\beta = 0.20^{o}$ (solid lines), 0.25^{o} (dotted lines), 0.30^{o} (dashed lines) and 0.35^{o} (dashed-dotted lines) at f = 45 GHz and $\varphi = 45^{o}$. (a) Main lobe (b) side lobes at $\theta = -0.15^{o}$ to -0.045^{o} and (c) side lobes at $\theta = 0.045^{o}$ to 0.15^{o}

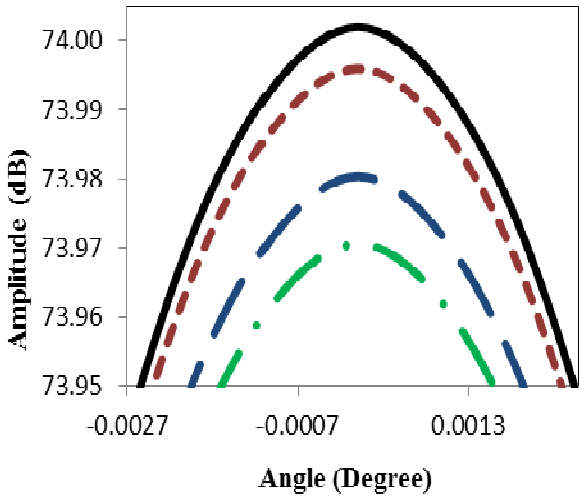

(a)

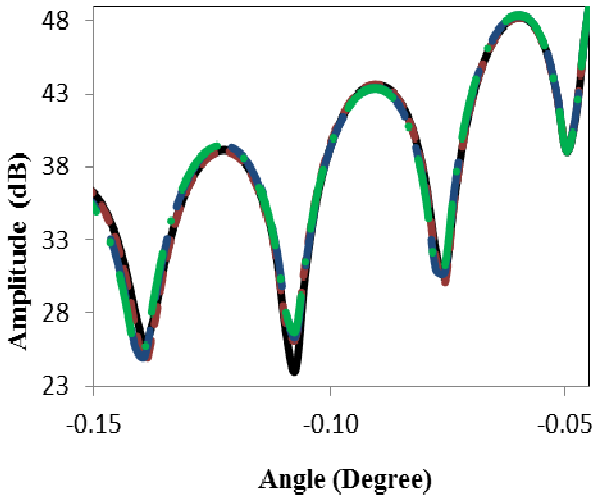

(b)

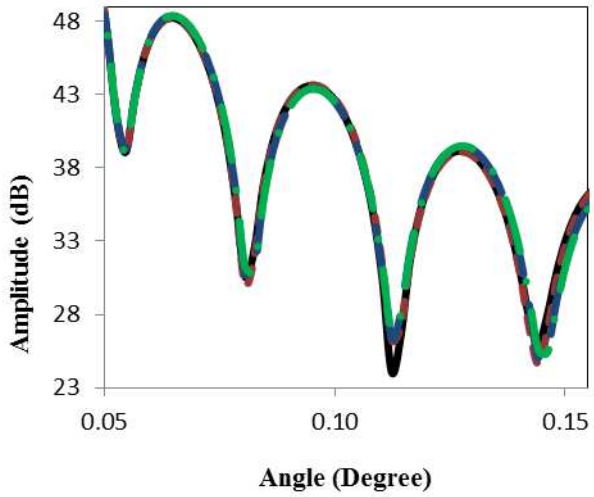

(c)

Fig. 4 The beam patterns of an offset Cassegrain with $\beta = 0.20^{o}$ (solid lines), 0.25^{o} (dotted lines), 0.30^{o} (dashed lines) and 0.35^{o} (dashed-dotted lines) at f = 45 GHz and $\varphi = 90^{o}$. (a) Main lobe (b) side lobes at $\theta = -0.15^{o}$ to -0.045^{o} and (c) side lobes at $\theta = 0.045^{o}$ to 0.15^{o}

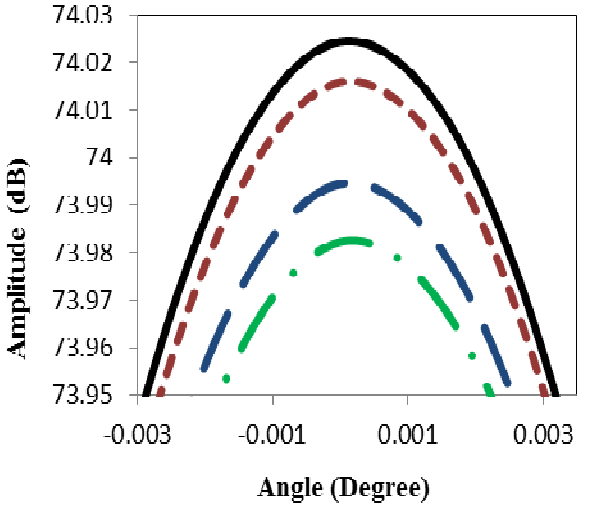

(a)

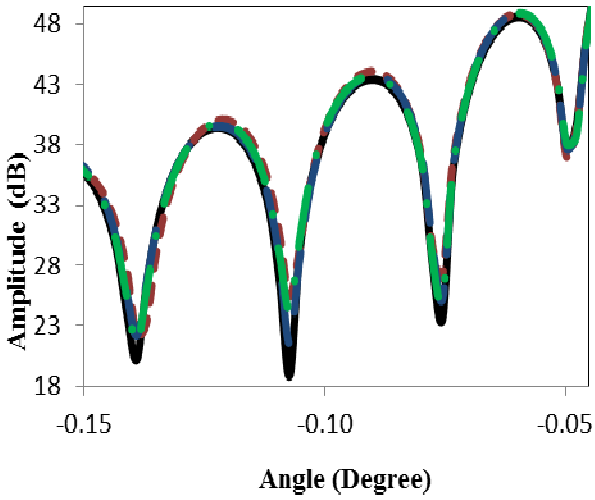

(b)

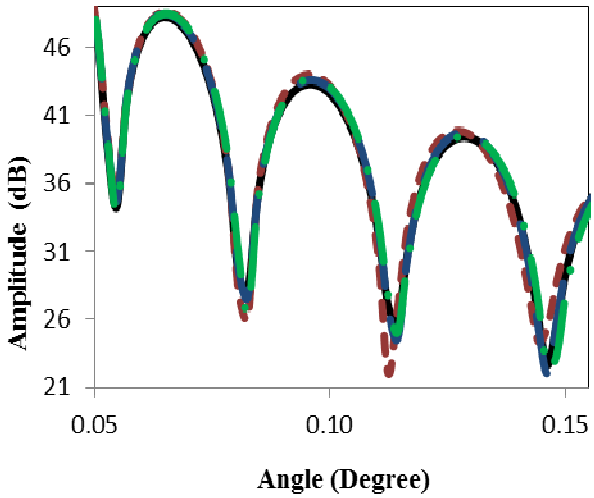

(c)

Fig. 5 The beam patterns of an offset Gregorian with $\beta = 0.20^{o}$ (solid lines), 0.25^{o} (dotted lines), 0.30^{o} (dashed lines) and 0.35^{o} (dashed-dotted lines) at f = 45 GHz and $\varphi = 0^{o}$. (a) Main lobe (b) side lobes at $\theta = -0.15^{o}$ to -0.045^{o} and (c) side lobes at $\theta = 0.045^{o}$ to 0.15^{o}

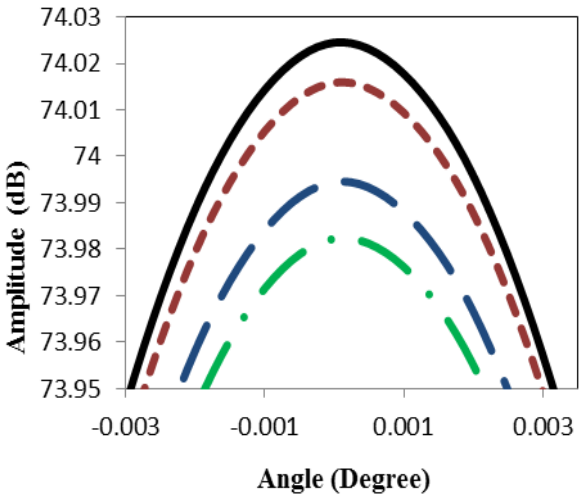

(a)

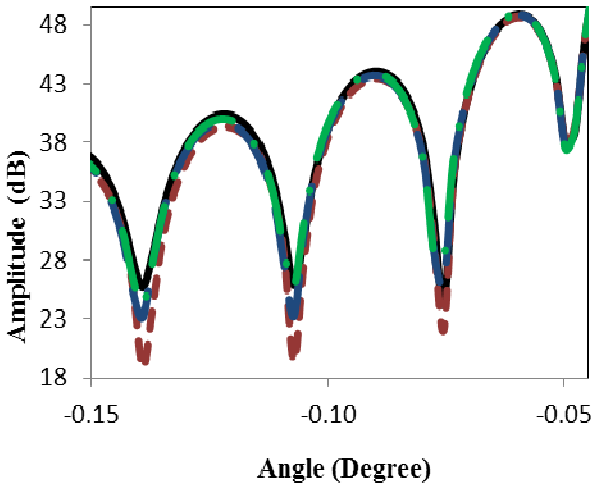

(b)

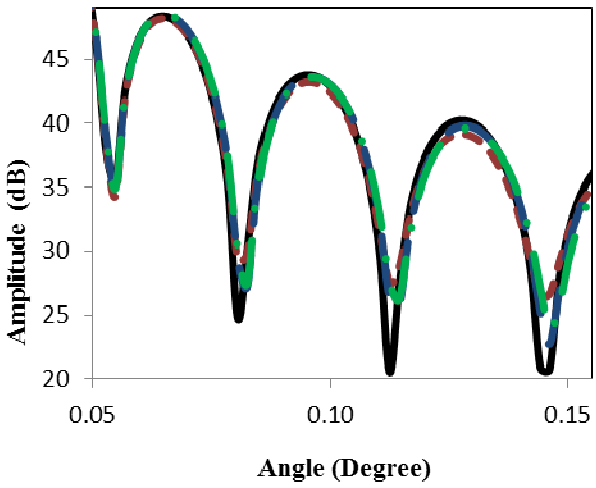

(c)

Fig. 6 The beam patterns of an offset Gregorian with β = 0.20° (solid lines), 0.25° (dotted lines), 0.30° (dashed lines) and 0.35° (dashed-dotted lines) at f = 45 GHz and φ = 45°. (a) Main lobe (b) side lobes at θ = -0.15° to -0.045° and (c) side lobes at θ = 0.045° to 0.15°

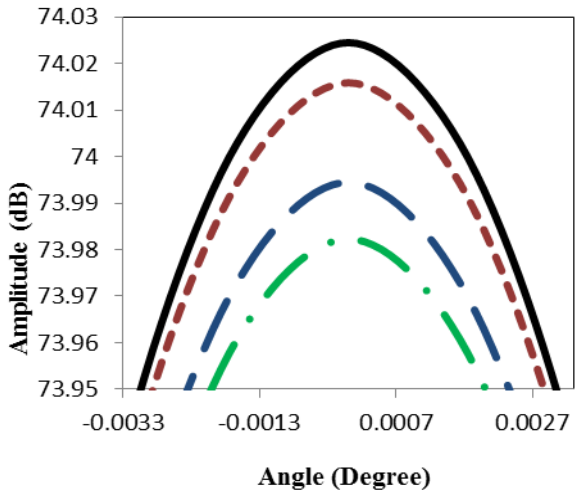

(a)

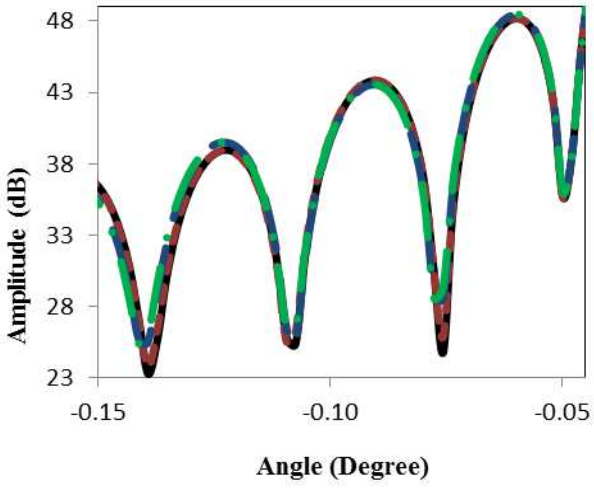

(b)

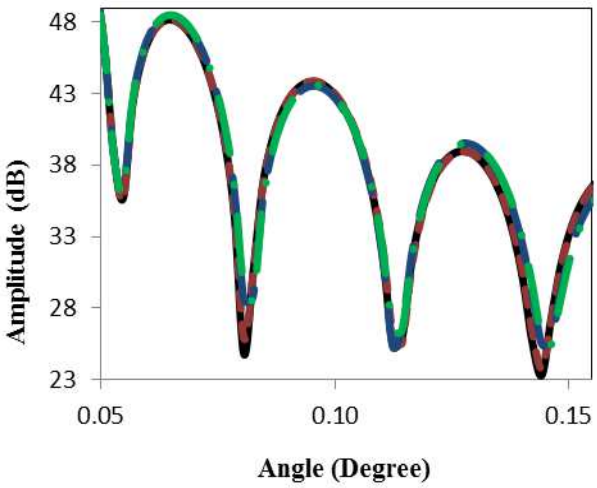

(c)

Fig. 7 The beam patterns of an offset Gregorian with β = 0.20° (solid lines), 0.25° (dotted lines), 0.30° (dashed lines) and 0.35° (dashed-dotted lines) at f = 45 GHz and φ = 90°. (a) Main lobe (b) side lobes at θ = -0.15° to -0.045° and (c) side lobes at θ = 0.045° to 0.15°

Since it is interesting to determine which of the two offset reflectors perform better, we compare the radiation patterns of both the Cassegrain and Gregorian configurations at β = 0.20°. As shown in Fig. 8 to 10, the side lobes of the

two offset antennas are in close proximity. However, the main lobe of the Gregorian design is relatively higher than its Cassegrain counterpart. The amplitude at the main lobe of the Gregorian configuration is approximately 74.02 dB, while that of the Cassegrain configuration is approximately 74 dB. Similarly, the amplitude at the highest side lobe of the Gregorian configuration is approximately 48.4 dB, whereas, that of the Cassegrain configuration is approximately 48.5 dB. The maximum (relative) side lobe level, SLL_{dB} is given by [23].

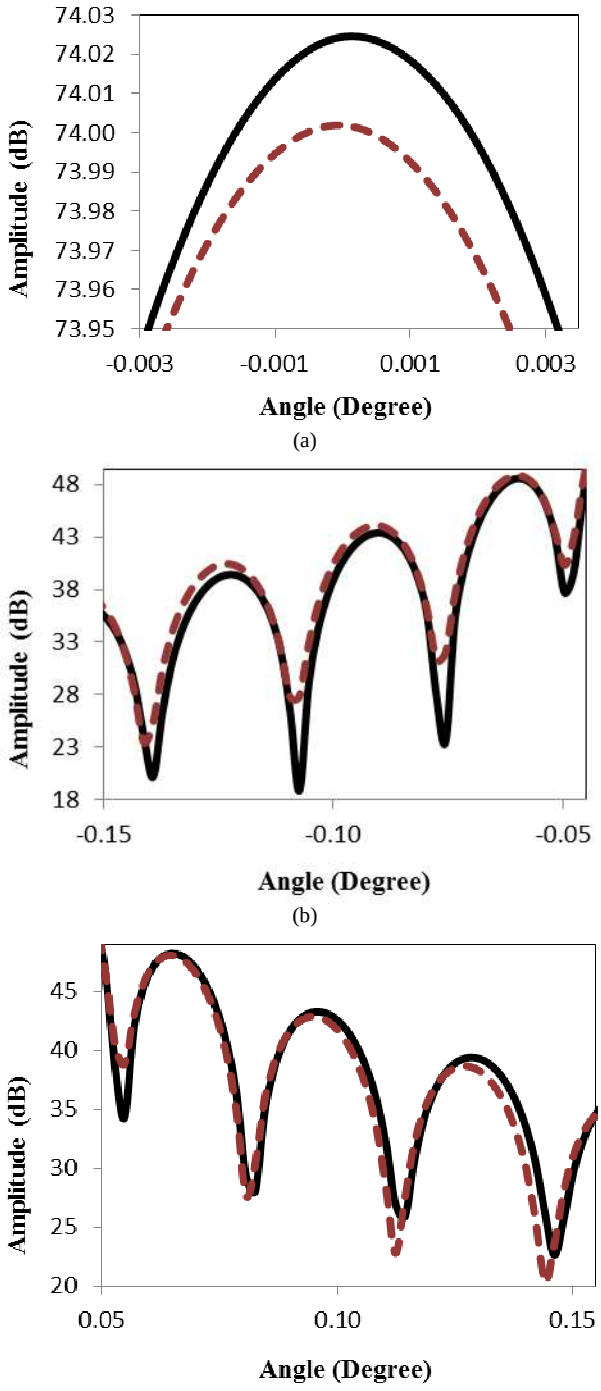

Fig. 8 The beam patterns of an offset Cassegrain (dashed lines) and Gregorian (solid lines) configuration at f = 45 GHz and φ = 0°. (a) Main lobe (b) side lobes at θ = -0.15° to -0.045° and (c) side lobes at θ = 0.045° to 0.15°

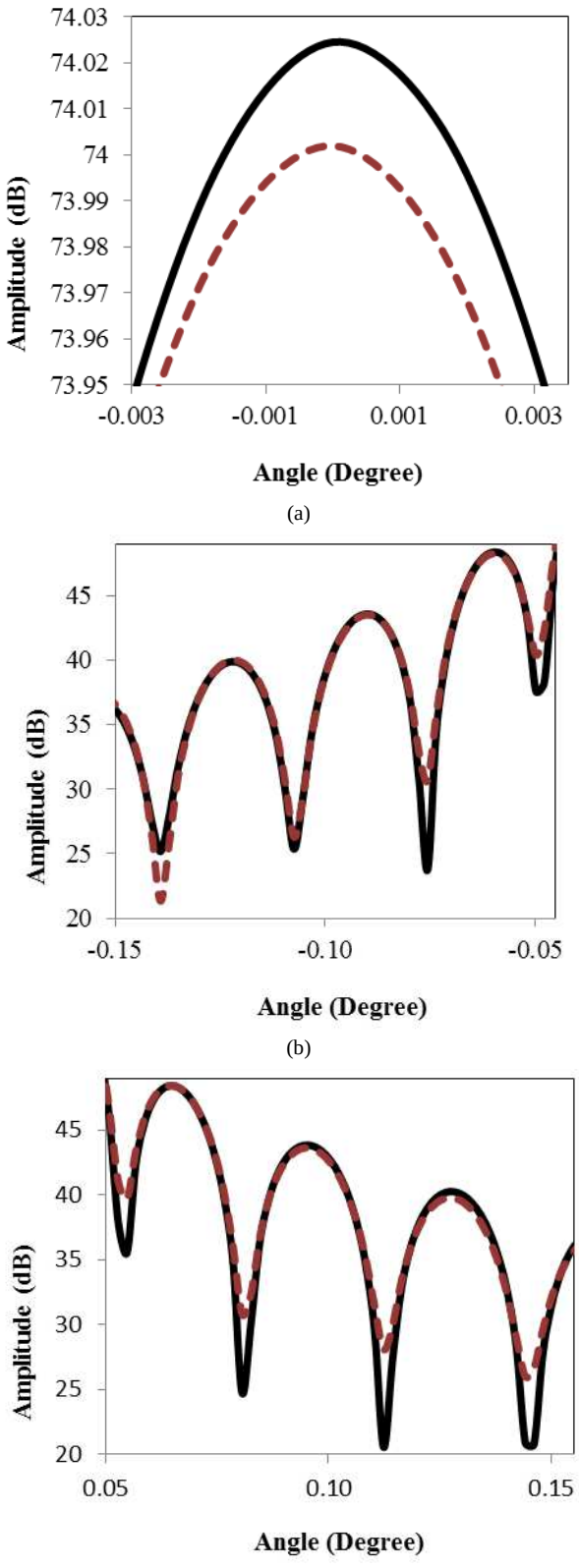

Fig. 9 The beam patterns of an offset Cassegrain (dashed lines) and Gregorian (solid lines) configuration, at f = 45 GHz and φ = 45°. (a) Main lobe (b) side lobes at θ = -0.15° to -0.045° and (c) side lobes at θ = 0.045° to 0.15°

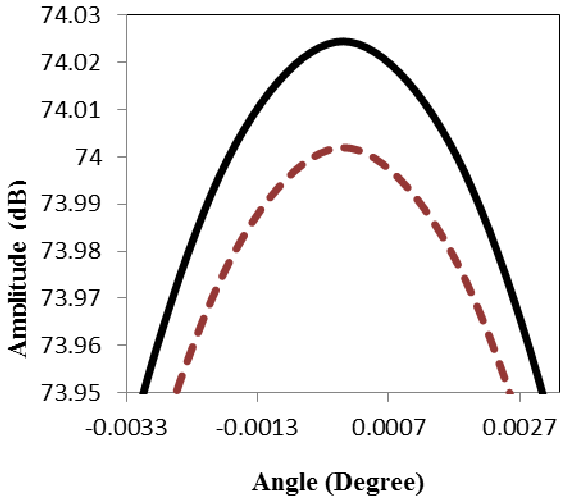

(a)

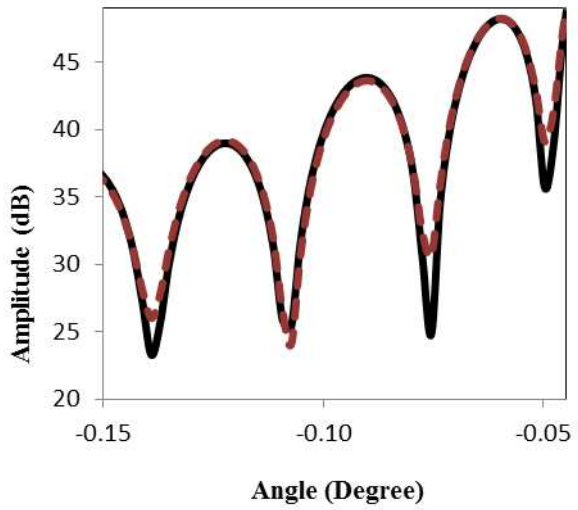

(b)

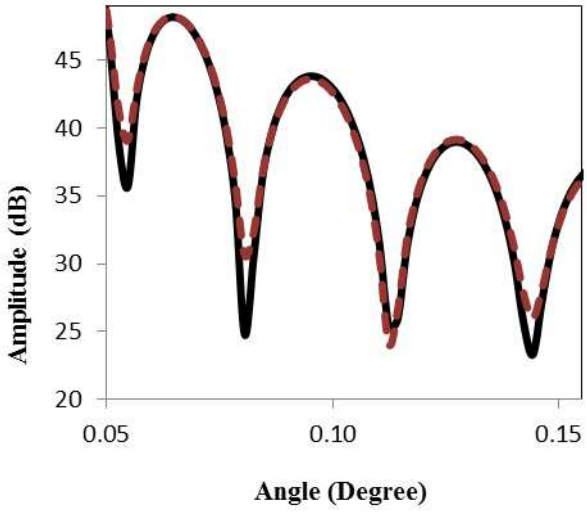

(c)

Fig. 10 The beam patterns of an offset Cassegrain (dashed lines) and Gregorian (solid lines) configuration, at f = 45 GHz and φ = 90°. (a) Main lobe (b) side lobes at θ = -0.15° to -0.045° and (c) side lobes at θ = 0.045° to 0.15°

$$SLL_{dB} = 20\log\left|\frac{F(SLL)}{F(max)}\right| \quad (2)$$

where |F(max)| is the maximum value of the pattern magnitude, i.e. the peak of the main lobe and |F(SLL)| is the maximum pattern value of the highest side lobe. The SLL_{dB} for the Cassegrain and Gregorian configurations are found, respectively, as -3.67 dB and -3.69 dB. It is apparent that the Gregorian configuration has lower maximum side lobe level. In other words, the Gregorian configuration performs relatively better than its Cassegrain counterpart. Although the main lobe is relatively higher in the Gregorian design, it can be observed that the power received in both configurations is still very close in magnitude.

IV. Conclusions

We have performed a comparison between two popular dual offset antenna designs, i.e. the offset Cassegrain and Gregorian reflectors. To reduce spillover loss, we have adjusted the angle between the axis of the primary reflector and that of the sub-reflector to 0.20°. This is to ensure that the feed is close enough and yet not being blocked by the primary reflector. From the results, it is observed that the radiation patterns generated from both antenna configurations are in close proximity to each other. Nonetheless, the Gregorian design shows relatively higher magnitude at the main lobe which indicating that it gives better performance than its Cassegrainian counterpart.

Acknowledgment

Part of this work has been supported by the Fundamental Research Grant Scheme (FRGS funded by the Ministry of Education, Malaysia (project: FRGS/2/2013/SG02/UTAR/02/1).

References

[1] H. A. Ford and J. Bregman, "A green bank telescope search for highly extended HI disks around spiral galaxies," *IAU General Assembly*, vol. 22, pp. 57205, Aug. 2015.

[2] K. H. Yeap, C. Y. Tham, K. C. Yeong, K. H. Chong, Z. I. Rizman and C. C. Yang, "Analysis of normal and superconducting coplanar waveguides in radio astronomy," *International Journal of Electronics, Computer, and Communication Technologies*, vol. 2, pp. 9-12, 2011.

[3] J. C. Cheng, E. S. Cheng, D. A. Cottingham, R. E. Eplee, Jr., D. J. Fixsen, T. Hewagama, R. B. Isaacman, K. A. Jensen, S. S. Meyer, P. D. Noerdlinger, S. M. Read, L. P. Rosen, R. A. Shafer, E. L. Wright, C. L. Bennett, N. W. Boggess, M. G. Hauser, T. Kelsall, S. H. Moseley, Jr., R. F. Silverberg, G. F. Smoot, R. Weiss and D. T. Wilkinson, "Measurement of the cosmic microwave background spectrum by the COBE FIRAS instrument," *The Astrophysical Journal*, vol. 410, pp. 439-444, Jan. 1994.

[4] K. H. Yeap, Y. H. Law, Z. I. Rizman, Y. K. Cheong, C. E. Ong and K. H. Chong, "Performance analysis of paraboloidal reflector antennas in radio telescopes," *International Journal of Electronics, Computer, and Communication Technologies*, vol. 4, pp. 21-25, 2013.

[5] A. Wotten, "ALMA capabilities for observations of spectral line emission," *Astrophysics and Space Science*, vol. 313, pp. 9-12, 2008.

[6] K. H. Yeap, C. Y. Tham, H. Nisar and S. H. Loh, "Analysis of probes in a rectangular waveguide," *Frequenz*, vol. 67, pp. 145-154, Apr. 2013.

[7] K. H. Yeap, C. Y. Tham, G. Yassin and K. C. Yeong, "Attenuation in rectangular waveguides with finite conductivity walls," *Radioengineering*, vol. 20, pp. 472-478, 2011.

[8] S. Paine, D. C. Papa, R. L. Leombruno, X. Zhang and R. Blundell, "Beam waveguide and receiver optics for the SMA," in *Proc. ISSTT'94*, 1994, p. 811-823.

[9] C. A. Balanis, *Antenna Theory: Analysis and Design*, 4th ed., New York, USA: John Wiley and Sons, 2016.

[10] T. L. Wilson, K. Rohlfs and S. Huttemeister, *Tools of Radio Astronomy: Astronomy and Astrophysics Library*, 6th ed., Berlin, Germany: Springer-Verlag, 2014.

[11] J. L. Han, P. B. Demorest, W. V. Straten and A. G. Lyne, "Polarization observations of 100 pulsars at 774 MHz by the green bank telescope," *The Astrophysical Journal Supplement Series*, vol. 181, pp. 557-571, Mar. 2009.

[12] S. M. Ransom, P. S. Ray, F. Camilo, M. S. E. Roberts, O. Celik, M. T. Wolff, C. C, Cheung, M. Kerr, T. Penucci, M. E. Decesar, I. Cognard, A. G. Lyne, B. W. Stappers, P. C. C. Freire, J. E. Grove, A. A. Abdo, G. Desvignes, D. Donato, E. C. Ferrara, N. Gehrels, L. Guillemot, C. Gwon, A. K. Harding, S. Johnston, M. Keith, M. Kramer, P. F. Michelson, D. Parent, P. M. S. Parkinson, R. W. Romani, D. A. Smith, G. Theureau, D. J. Thompson, P. Weltevrede, K. S. Wood and M. Ziegler, "Three millisecond pulsars in Fermi Lat unassociated bright sources," *The Astrophysical Journal Letters*, vol. 727, pp. 1-6, Dec. 2011.

[13] T. R. Hunter, F. R. Schwab, S. D. White, J. M. Ford, F. D. Ghigo, R. J. Maddalena, B. S. Mason, J. D. Nelson, R. M. Prestage, J. Ray, P. Ries, R. Simon, S. Srikanth and P. Whiteis, "Holographic measurement and improvement of the green bank telescope surface," *Publications of the Astronomical Society of the Pacific*, vol. 123, pp. 1087-1099, Sep. 2011.

[14] R. M. Prestage, K. T. Constantikes, T. R. Hunter, L. J. King, R. J. Lacasse, F. J. Lockman and R. D. Norrod, "The green bank telescope," *Proceedings of the IEEE*, vol. 97, pp. 1382-1290, 2009.

[15] I. Seker, J. D. Mathews, J. Wiig, P. F. Gutierrez, J. S. Friedman and C. A. Tepley, "First results from the Penn state allsky imager at the Arecibo observatory," *Earth Planets Space*, vol. 59, pp. 165-176, Mar. 2007.

[16] J. D. Mathews, J. Doherty, C. –H. Wen, S. J. Briczinski, D. Janches and D. D. Meisel, "An update on UHF radat meteor observations and associated signal processing techniques at Arecibo observatory," *Journal of Atmospheric and Solar-Terrestrial Physics*, vol. 65, pp. 1139-1149, Jul. 2003.

[17] A. P. V. Siemion, G. C. Bower, G. Foster, P. L. McMahon, M. I. Wagner, D. Werthimer, D. Backer, J. Cordes and J. V. Leeuwen, "The Allen telescope array fly's eye survey for fast radio transients", *The Astrophysical Journal*, vol. 744, pp. 1-12, Dec. 2012.

[18] S. Croft, G. C. Bower, G. Keating, C. Law, D. Whysong, P. K. G. Williams and M. Wright, "The Allen telescope array twenty-centimeter survey-A 700-square-degree, multi-epoch radio data set. II. Individual epoch transient statistics," *The Astrophysical Journal*, vol. 731, pp. 1-11, Mar. 2011.

[19] W. Rusch, "The current state of the reflector antenna are-entering the 1990s," *Proc. of the IEEE*, vol. 80, pp. 113-126, Jan. 1992.

[20] J. S. Courtney-Pratt, J. H. Hett and J. W. McLaughlin, "Optical measurements on Telstar to determine the orientation of the spin axis, and the spin rate," *Journal Society of Motion Picture and Television Engineers*, vol. 72, pp. 462-484, Jun. 1963.

[21] G. Shaker, S. Safavi-Naeini and N. Sangary, "Modern antenna design using mode analysis techniques," *Progress In Electromagnetics Research B*, vol. 62, pp. 153-165, 2015.

[22] K. B. Kong, H. S. Kim, R. S. Aziz and S. O. Park, "Design of offset dual-reflector antennas for improving isolation level between transmitter and receiver antennas," *Progress In Electromagnetics Research C*, vol. 57, pp. 193-203, 2015.

[23] W. L. Stutzman and G. A. Thiele, *Antenna Theory and Design*, 2nd ed., New Delhi, India: Wiley India Pvt. Ltd., 2015.